Heliyon 10 (2024) e23930

Contents lists available at ScienceDirect

Heliyon

journal homepage: www.cell.com/heliyon

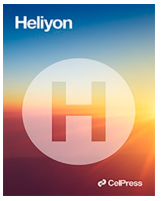

In-depth analysis of prognostic markers associated with the tumor immune microenvironment and genetic mutations in breast cancer based on an NK cell-related risk model

Dongmin Yu [a,1,*], Chao Huang [b,1], Luochen Zhu [c,1], Yuxi Wei [d], Meifang Li [a,**]

[a] Department of Breast Disease Comprehensive Center, First Affiliated Hospital of Gannan Medical University, Ganzhou, 341000, People's Republic of China
[b] Nail and Breast Surgery, Suqian First People's Hospital, Suqian, 223800, People's Republic of China
[c] Department of Pharmacy, Tumor Hospital Affiliated to Nantong University, Nantong, 226361, People's Republic of China
[d] First Clinical Medical College of Gannan Medical College, Ganzhou, 341000, People's Republic of China

ARTICLE INFO

Keywords:
Natural killer cell
Breast cancer
IFNE
Prognosis

ABSTRACT

The natural killer (NK) cell population is unique because it consists of innate lymphocytes capable of detecting and eliminating tumors and virus-infected cells. This research aims to identify a new prognostic signal in breast cancer (BRCA) based on NK-cell-related genes (NKRGs). A variety of sequencing and gene mutation data, along with clinical information, were collected from The Cancer Genome Atlas (TCGA) and Gene Expression Database (GEO). COX regression and least absolute shrinkage and selection operator (LASSO) Cox regression analyses were conducted to identify prognostic genes. In addition, the immune-related analysis was performed to evaluate the association between the immune microenvironment and clusters and risk model. The Edu assay, colony assay, wound healing assay, and transwell assay were performed to evaluate the cell proliferative and invasive abilities. A 4-NKRG-based prognostic model was constructed. Patients in high-risk groups were associated with poorer OS in TCGA and GSE42568. Further, a nomogram was constructed for better prediction of the prognosis of patients with BRCA. Finally, it was discovered that the over-expression of IFNE could suppress the proliferative and invasive abilities of BRCA cells, which might be a promising biomarker for patients with BRCA. As a result, we developed a novel 4-NKRG signal and nomogram capable of predicting the prognosis of patients with BRCA. Additionally, this model was closely associated with the immune microenvironment, which opened new therapeutic avenues for the treatment of cancer in the future.

1. Introduction

Breast cancer (BRCA) is the most common type of cancer and the leading cause of cancer-associated death in women worldwide [1], despite enormous efforts to develop effective treatment strategies [2]. It is often difficult to classify BRCA as a single disease due to its heterogeneity. The heterogeneous nature of BRCA has been known since the 19th century and has dictated the classification of the

* Corresponding author.
** Corresponding author.
E-mail addresses: 18370955568@163.com (D. Yu), meifang_li@gmu.edu.cn (M. Li).
[1] These authors contributed equally: Dongmin Yu, Huang Chao and Luochen Zhu.

https://doi.org/10.1016/j.heliyon.2023.e23930
Received 6 August 2023; Received in revised form 28 November 2023; Accepted 15 December 2023
Available online 22 December 2023

disease [3]. Spatial and temporal heterogeneities have been found between patients with BRCA as well as within single tumors [4]. Spatial heterogeneity involves differences in phenotypic, transcriptomic, epigenetic, and genomic features within a tumor [5]. Temporal heterogeneity involves differences between primary tumors and metastases or between different metastatic sites over time during tumor progression [6]. It is important to note that even the tumor microenvironment (TME) can contribute to tumor heterogeneity, as it is affected by spatial heterogeneity within the tumor [7].

As innate lymphocytes are able to detect and eliminate tumor and virus-infected cells, natural killer (NK) cells constitute a unique population [8]. In addition to their cytotoxic effects, NK cells can also modulate immune responses through the production of cytokines [9]. The goal of NK cell-based therapies is to enhance NK cell potency and persistence by enhancing co-stimulatory signaling, inhibiting checkpoints, and increasing cytokine production [10]. Due to their ability to affect dendritic cells, macrophages, and neutrophils by producing cytokines and chemokines, NK cells are also termed "immunomodulatory" [11].

Over recent years, numerous studies have explored the relationship between NK cells and BRCA. One study revealed that immunosuppression in the TME of patients with BRCA directly worsens phenotype and suppresses NK cell function [12]. The NK cell-activating receptor DNAM-1 is liganded by CD155. The presence of m-CD155 and NK-TIL is associated with a good prognosis in patients with BRCA, whereas the presence of cyt-CD155 is associated with a poor prognosis [13]. According to another study, mastectomy may increase NK cell activity in patients with BRCA, which may produce positive therapeutic effects [14].

Recently, with the development of bioinformatics, numerous studies have applied bioinformatics analyses to identify potential biomarkers for better diagnosis and prognosis of patients with BRCA [15–17]. The present work aimed to explore the behavior of NK cells in BRCA and identify potential biomarkers for NK cell-based BRCA immunotherapy.

2. Materials and methods

2.1. Dataset downloading for patients with BRCA

Data from RNAseq analysis and corresponding clinical information for BRCA were obtained from The Cancer Genome Atlas (TCGA) dataset (available at http://portal.gdc.com). The dataset contained data for 113 normal tissues and 1113 tumor tissues with BRCA. An additional data set was sourced from the GEO database (Gene Expression Omnibus, https://www.ncbi.nlm.nih.gov/geo/) in MINiML format. The GSE included all platforms, samples, and GSE records. Based on the corresponding platform annotation information, the average value of all genes associated with multiple probes for the probe IDs corresponding to multiple platforms. The GSE42568 cohort, covering 104 patients with BRCA, served as an external validation cohort.

2.2. Identification of the differentially expressed genes in the BRCA cohort

To identify differentially expressed mRNAs, the Limma package of the R programming language was used. The threshold for detecting differential mRNA expression was defined as follows: "P value < 0.05 with log2 (fold change) > 0.5 or log2 (fold change) < -0.5."

2.3. Protein-protein interaction (PPI) network

To determine interactions between genes and proteins involved in BRCA, a protein-protein interaction (PPI) network was constructed using STRING (https://www.string-db.org/).

2.4. Pathway enrichment analysis

Functional enrichment was performed to further validate the functions of the potential key genes. Gene Ontology (GO) was a useful tool for annotating genes with functions, such as molecular functions (MFs), biological pathways (BPs), and cellular components (CCs). KEGG pathway enrichment was a practical way to gain deep insights into the function of genes and the genome. ClusterProfiler in the R software was used to analyze GO functions and enrich pathways related to mRNAs showing prognostic potential for BRCA.

2.5. Gene somatic mutation analysis

Data on patients with BRCA regarding mutant MAF were obtained from the TCGA dataset. Using the R software package maftools somatic mutations in patients were downloaded from the BRCA cohort and visualized.

2.6. Immune cell infiltration analysis

To achieve robust immune score estimation, several algorithms, including TIMER, xCell, MCP-counter, CIBERSORT, EPIC, CIBERSORT-ABS, and QUANNTISEQ were used [18–23]. Upon systematically benchmarking these algorithms, each algorithm had its own unique characteristics and strengths. In addition, the potential immunotherapy response was predicted using CTLA 4 and PD 1 scores, using the online tool TIDE (http://tide.dfci.harvard.edu/) [24].

2.7. Construction of an NK cell-based prognostic prediction model in the BRCA cohort

Based on counts data and clinical information of patients with BRCA, a regression algorithm called the Least Absolute Shrinkage and Selection Operator (LASSO) was used, along with a 10-fold cross-validation process for feature selection. Prognostic models were constructed using univariate and multivariate Cox regression analyses, and the survival package in R software was used for analysis. The log-rank test was implemented to determine survival differences between two or more of the abovementioned groups using KM survival analysis.

2.8. Subgroup analysis

The R package ConsensusClusterPlus was used for consistency analysis. The maximum number of clusters was nine, and 80 % of the total samples were extracted 100 times, using clusterAlg = "hc" and innerLinkage = "ward.D2″

2.9. Subgroup- and prognosis prediction model-based correlation analysis

Data on the expression levels of immune checkpoint-related genes and human leukocyte antigen (HLA) genes and clinical characteristics were extracted from the TCGA database. The correlation analysis was performed using the R software packages ggplot 2 and pheatmap.

2.10. Cell culture

BRCA cell lines MDA-MB-231, BT-549, ZR-75-1, MCF-7, and SK-BR-3 and breast normal cell lines Hs 578Bst were obtained from the Institute of Biochemistry and Cell Biology of the Chinese Academy of Sciences (Shanghai, China). The cells were cultivated in DMEM or DMEM/F12 (Life, Shanghai, China). Subsequently, the IFNE protein expression level was detected using Western blot analysis to confirm the successful construction of the cell line.

2.11. RNA purification and qRT-PCR

The total RNAs from tissue samples (approximately 3.0 g) or cells (1×10^6) or cells in Trizol (Invitrogen, United States) were extracted. The ultraviolet spectrophotometry technique was used to determine the concentration and purity of total RNA at 260 nm and 280 nm. A reverse transcription kit (Thermo Fisher Scientific, Inc.) was used to convert RNA into cDNA. The protocol outlined by the manufacturer was followed to conduct the experiments. The qPCR technique was used to study the samples using SYBR Green Master (TsingKe, China). GAPDH served as the endogenous control of IFNE. The primers used in this study are listed below:

IFNE forward, 5′-TCAGCCTCTTCAGGGCAAAT-3′, and reverse, 5′-CCAGTCCCATGAGTGCTTCT-3';

GAPDH forward, 5' -TAGATGACACCCGTCCCTGA-3′, and reverse, 5′-ACCTCCACCTGTCCTTAGTG -3'

2.12. Western blot analysis

Proteins obtained from cultured cells were subjected to electrophoresis, following which they were transferred onto polyvinylidene difluoride membranes. Subsequently, the samples were sealed using 5 % skimmed milk (time: 2 h) at room temperature. Afterward, the protein was incubated with the specific primary antibody. The sample was refrigerated overnight at 4 °C. Following incubation, the samples were washed three times with PBST, with each washing cycle lasting 10 min. Post-washing, the samples were incubated with the secondary antibody (Goat Anti-Rabbit IgG-HRP, 1:5,000, Abmart). Rabbit anti-IFNE (1:1,000, Thermo Fisher Scientific) and GAPDH (1:5,000, Abmart) antibodies were used for the experiments.

2.13. Transwell assay

A 24-well plate was divided into upper and lower chambers by integrating transwell chambers with a pore size of 8.0 mm. Then, 600 ml medium with 10 % fetal bovine serum (FBS) was added to the lower chamber, and 200 ml serum-free, conditioned medium containing 2×10^4 cells was added to the upper chamber. After 24 h, cells in the upper chamber were wiped with a cotton swab, and cells that had invaded the bottom surface of the chamber were fixed and stained with crystal violet.

2.14. Wound healing assay and CCK8 assay

Following transfection, BT-549 cells were cultured in 6-cm dishes until they reached 90%–95 % confluency. A wound was created down the middle of the cell monolayer by scratching with a 200 ml tip. Unattached cells were then washed using PBS (Gibco). The wound was photographed at 0 h and 24 h to evaluate the proliferation and metastasis of BT-549 cells.

By counting the viable cells remaining after the CCK-8 assay, the viability of cells was determined. Briefly, BT-549 cells were seeded

in 96-well plates at a cell density of 3000 cells per well and incubated for 24 h. Then, 10 μl of CCK-8 reagent was added to the culture medium in each well, and the plates were incubated at 37 °C for 2 h. An automatic microplate reader (Synergy 4; BioTek, Winooski, VT, USA) was then used to measure light absorbance six times per well at 450 nm.

2.15. Colony formation assay and 5-Ethynyl-2′ -deoxyuridine (EdU) staining

For the colony-forming assay, cells were treated with plasmids or irradiated at 0, 4, or 8 Gy for 24 h to determine their ability to

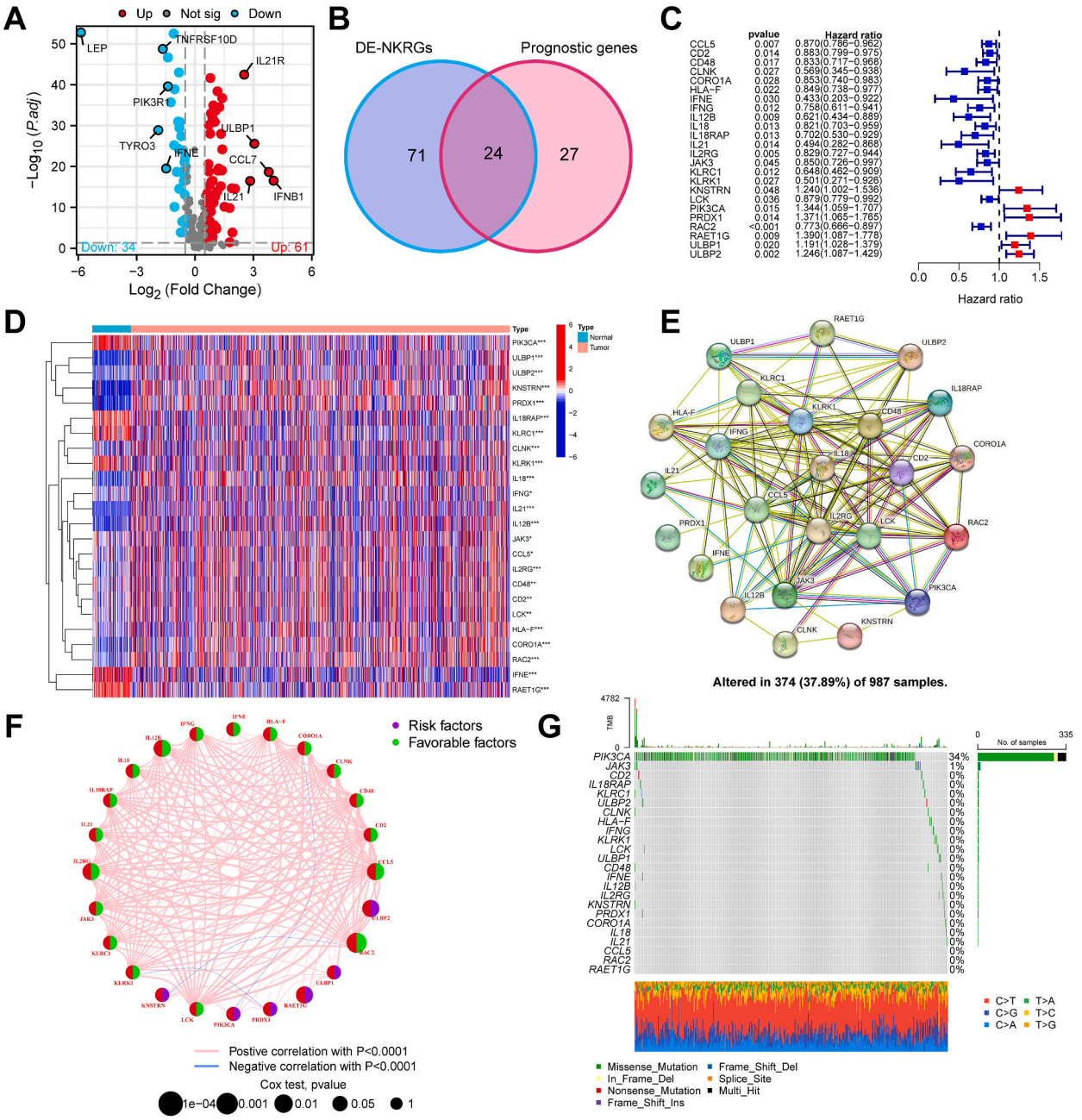

Fig. 1. Identification of the role of NKRGs in a breast cancer cohort. (A) The volcano map demonstrates the differentially expressed NKRGs identified in our breast cancer cohort. (B) The Venn diagram shows the NKRGs that are highly associated with breast cancer prognosis and differentially expressed in breast cancer. (C) Univariate cox regression analysis based on the 24 prognosis-related NKRGs. (D) Heatmap showing the expression levels of the 24 prognosis-related NKRGs identified in the breast cancer cohort. (E) PPI network based on the 24 prognosis-related NKRGs. (F) Network demonstrating the risk or favorable factors and interactive correlations between 24 prognosis-based NKRGs. (G) Somatic mutation analysis in the whole TCGA cohort. Data are analyzed by Wilcoxon test.

form colonies. After 14 days, the colonies formed were counted.

To detect cells that retained EdU, DMSO was added to culture flasks containing BT-549 cells before their incubation overnight with 0.1 % EdU and Apollo staining solution (RiboBio).

2.16. Statistical analysis

Statistical analysis was carried out using the R programming language. Overall survival (OS) was determined using Kaplan-Meier survival curves and the log-rank test. Spearman correlation was conducted to identify the correlation between risk score and immune cell infiltration. Wilcox's signed-rank test was used to compare the proportions of tumor-infiltrating immune cells, immune

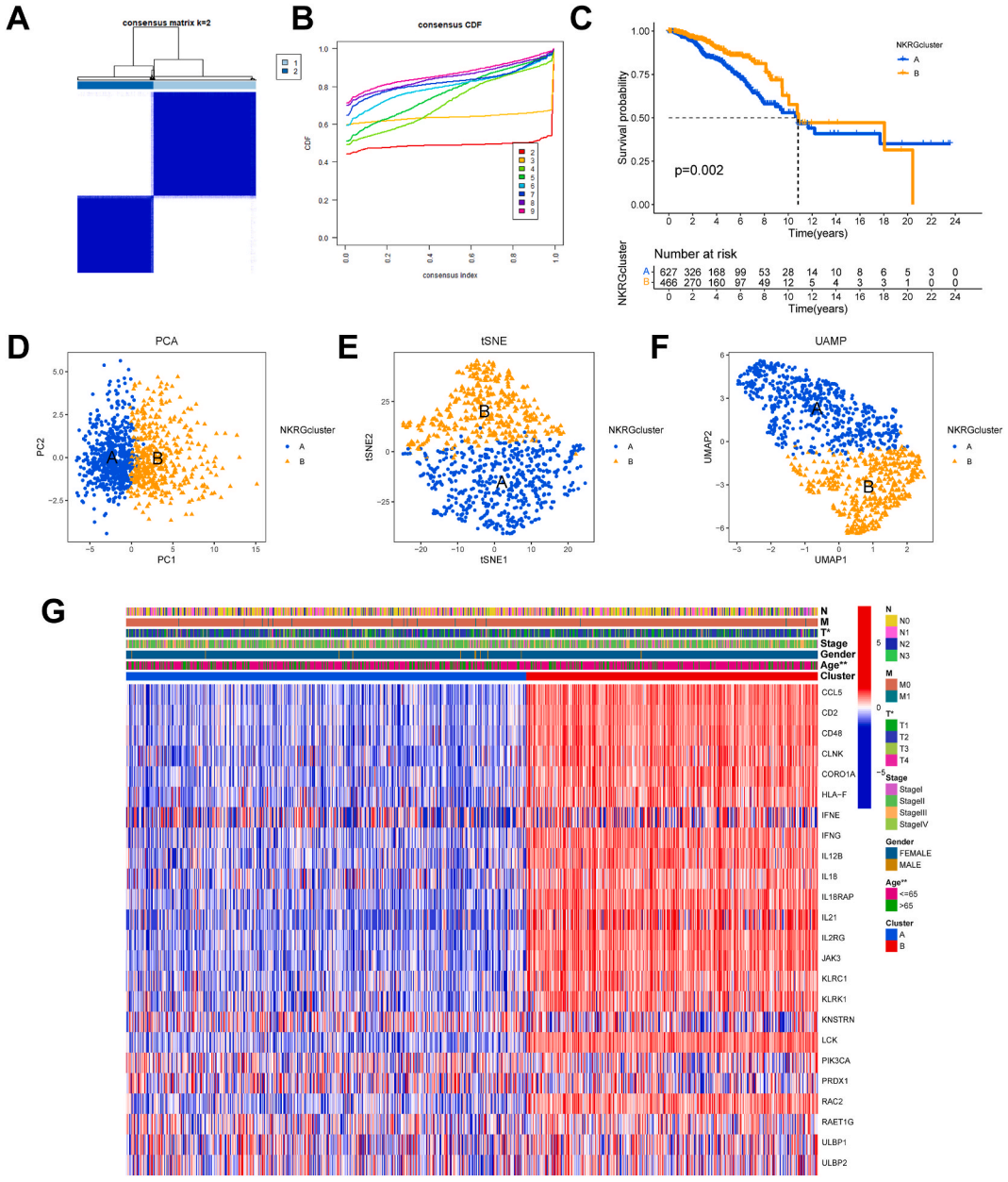

Fig. 2. Potential correlation between NKRG clusters and OS and clinical characteristics, immune-related indexes, pathways enriched in breast cancer, and somatic mutations. (A) Cluster diagram for the subtype analysis of breast cancer samples. Intragroup correlations were high and inter-group correlations were low at k = 2. (B) CDF curve of consensus cluster analysis. (C) Survival analysis comparison between NKRG cluster A and cluster B; Results obtained using the PCA (D), Tsne (E), and UAMP (F) dimensionality reduction algorithms. (G) Heatmap of clinical correlation analysis results. Data are analyzed by Wilcoxon test.

checkpoints, HLA-related genes, and clinical characteristics between the two groups.

3. Results

3.1. Correlation between NK cell-related genes and prognosis, somatic mutations, the PPI network, and BRCA cohort

First, we identified 244 genes on the ImmPort portal (https://www.immport.org/resources) that were related to the molecular characteristics of NK cells and the Molecular Signature Database (MSigDB) (Table S1). These genes were considered NK cell-related genes (NKRGs). Subsequently, 95 differentially expressed NKRGs were identified in BRCA (Fig. 1A, Table S2). Moreover, 51 NKRGs were closely associated with the prognosis of patients with BRCA. The Venn diagram constructed between these two sets of NKRGs demonstrated that 24 NKRGs were highly correlated with BRCA prognosis and were differentially expressed in BRCA (Fig. 1B). Next, a univariate Cox regression analysis of these 24 genes was performed (Fig. 1C, Table S3). The heatmap demonstrated the differential expression levels of these genes between healthy individuals and the BRCA cohort (Fig. 1D). Additionally, the PPI network constructed revealed strong positive relationships between the 24 genes (Fig. 1E). Among the 24 genes, six showed protective roles in BRCA, including ULBP2, ULBP1, RAET1G, PRDX1, and KNSTRN, and others were identified as risk factors (Fig. 1F). Finally, we identified mutations in 24 NKRGs, at a rate of 37.89 %. The highest mutation rate (about 34 %) in the BRCA cohort was recorded for PIK3CA (Fig. 1G).

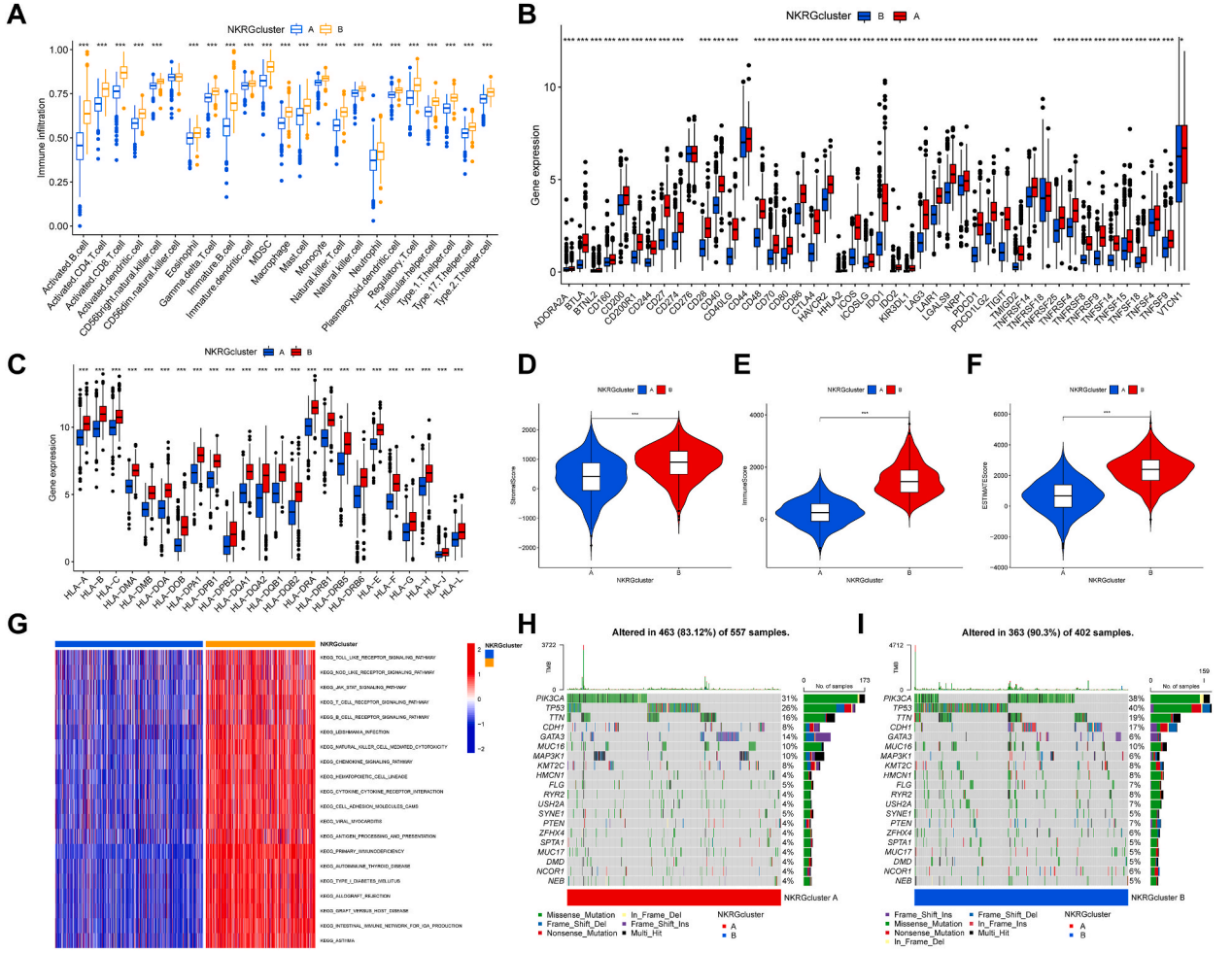

Fig. 3. Potential correlation between NKRG clusters and immune-related indexes, pathways enriched in breast cancer, and somatic mutations. (A) Correlation analysis between different NKRG clusters and immune-related cells. (B) Correlation analysis between different NKRG clusters and immune checkpoint-related genes. (C) Correlation analysis between different NKRG clusters and HLA-related genes. (D) Correlation analysis between different NKRG clusters and stromal score. (E) Correlation analysis between different NKRG clusters and immune score. (F) Correlation analysis between different NKRG clusters and estimate score. (G) KEGG pathway enrichment analysis comparison between the different NKRG clusters. (H) Somatic mutation analysis in NKRG cluster A; (I) Somatic mutation analysis in NKRG cluster B. Data are analyzed by Wilcoxon test.

3.2. Potential correlations between NKRG clusters and OS, clinical characteristics, immune-related indexes, enriched pathways, and somatic mutations in BRCA

To further explore the role of the 24 genes identified above in the BRCA cohort, a consensus cluster analysis was performed. The CDF curve obtained showed that, when k was equal to 2, the classification effect in the BRCA cohort was optimal (Fig. 2A–B and Fig. S1). Therefore, the 1093 patients with BRCA in the cohort were classified into NKRG cluster A (n = 627) and NKRG cluster B (n = 466) (Table S4). Subsequently, a survival analysis was performed. Patients with BRCA in NKRG cluster A were likely to have poorer OS (Fig. 2C). Moreover, using dimensionality reduction algorithms, the spatial distribution of patients with BRCA was visualized. The PCA, tSNE, and UAMP algorithms all suggested that the consensus cluster analysis demonstrated good effects (Fig. 2D–F). Next, a correlation analysis demonstrated that different T stages and ages of patients with BRCA were closely associated with different NKRG clusters (Fig. 2G and Fig. S2). Further, the correlation between various immune-related indexes and different NKRG clusters was evaluated. The immune cell infiltration analysis demonstrated that numerous immune-related cells, such as activated B cells, activated CD4 T cells, activated CD8 T cells, activated dendritic cells, and NK cells, were highly expressed in NKRG cluster B (Fig. 3A). Additionally, patients with BRCA in NKRG cluster B had high expression levels of numerous immune checkpoint-related genes, including ADORA2A, BTLA, BTNL2, CD160, CD200, CD244, CD27, and CD274 (Fig. 3B). These results suggested that patients with BRCA in NKRG cluster B exhibited better response to immune checkpoint therapy. Furthermore, patients with BRCA in NKRG cluster B have higher expression levels of HLA-related genes (Fig. 3C).

Subsequently, the correlation between the TME (TME) and different NKRG clusters was evaluated. Patients with BRCA in NKRG cluster B had higher stromal scores, immune scores, and estimate scores than those in NKRG cluster A (Fig. 3D–F). Additionally, different KEGG pathways, such as the toll-like receptor signaling pathway, nod-like receptor signaling pathway, JAK-STAT signaling pathway, T cell receptor signaling pathway, and B cell receptor signaling pathway, were observed to be closely associated with different NKRG clusters (Fig. 3G). The somatic mutation rates in NKRG cluster A and NKRG cluster B were 83.12 % and 90.3 %, respectively (Fig. 3H–I).

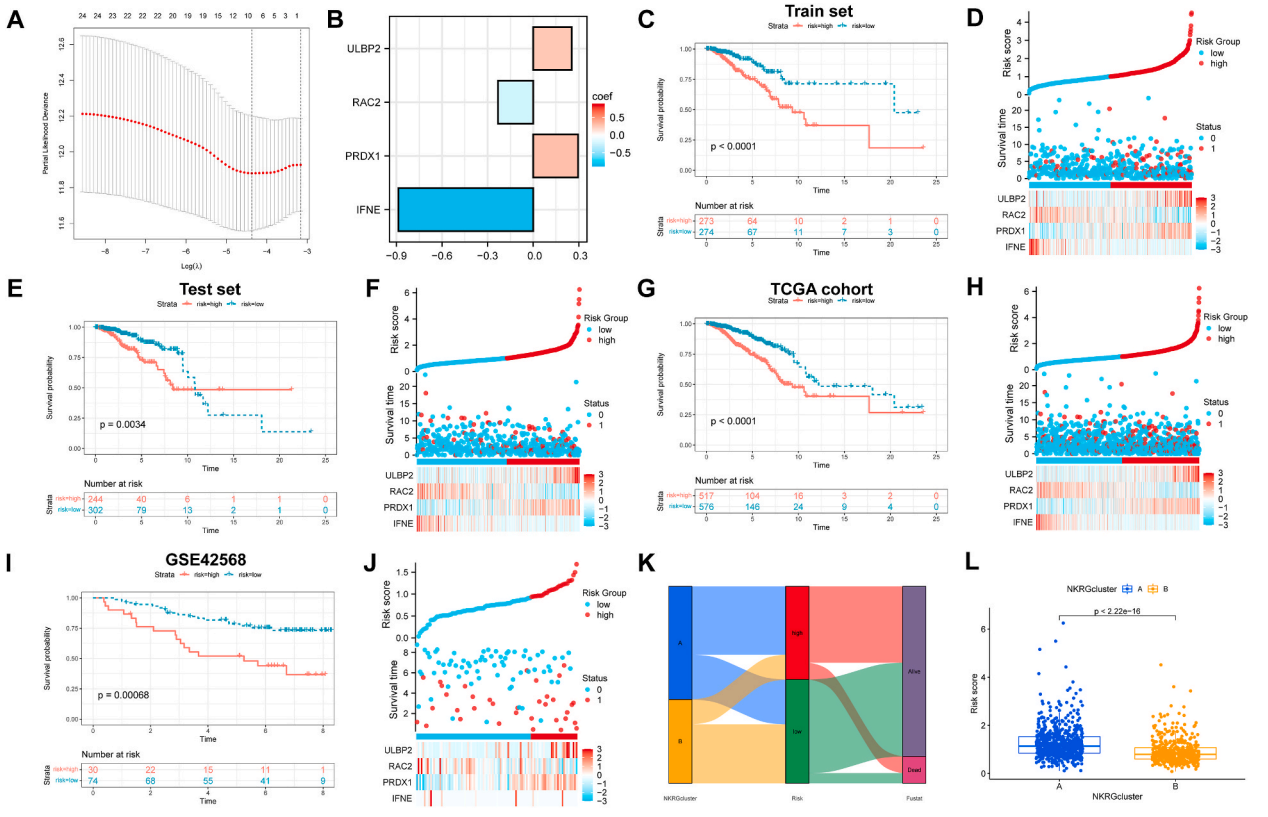

Fig. 4. NKRGs-based risk model (A) LASSO regression analysis. (B) Multivariate Cox regression analysis demonstrated that ULBP2, RAC2, PRDX1, and IFNE are closely associated with the prognosis of breast cancer patients; Survival analysis in the train set (C), test set (E), TCGA cohort (G), and GEO cohort (I). Risk plot for the train set (D), test set (F), TCGA cohort (H), and GEO cohort (J). (K) Sankey diagram showing the correlation between risk groups and different NKRG clusters. (L) Boxplot showing the correlation between risk groups and different NKRG clusters. Data are analyzed by Wilcoxon test.

3.3. Further exploration of the prognosis-related NKRGs in the BRCA cohort

First, patients with BRCA in the TCGA cohort were randomly divided into a train set and a test set. In the train set, LASSO regression analysis and multivariate Cox regression analysis were performed to identify prognosis-related NKRGs (Fig. 4A). Finally, four prognosis-related NKRGs (ULBPS, RAC2, PRDX1, and IFNE) were obtained (Fig. 4B). Next, each BRCA patient was assigned a risk score calculated as follows: Risk score = IFNE * −0.886752686232883 + PRDX1 * 0.294839736125548 + RAC2 * −0.231801327361253 + ULBP2 * 0.252737941352663 (Table S7). Subsequently, patients in the train set were equally divided into low- and high-risk groups based on their median risk score. Survival analysis showed that patients with higher risk scores in the train set, test set, whole TCGA cohort, and the GSE42568 external validation cohort had poorer OS (Fig. 4C, E, G, and I; Tables S5 and S6). BRCA patients were ranked from left to right according to the risk score that was calculated in different datasets, and the heatmaps indicated the four prognosis-related NKRGs in two risk groups (Fig. 4D, F and J). Moreover, the Sankey diagram and boxplot showed that patients with BRCA in NKRG cluster A were more likely to fall into the high-risk group (Fig. 4K-L). The ROC curve also demonstrated that the NKRG-based risk model showed good predictive value in the TCGA train set, the TCGA test set, the whole TCGA cohort, and the GSE42568 cohort (Fig. S3).

3.4. Correlation between clinical characteristics and NKRGs and construction of the BRCA cohort nomogram

A correlation analysis demonstrated that patients with high risk scores had a high stage and high T stage (Fig. 5A–G). Univariate independent prognosis analysis revealed that age, stage, T stage, M stage, N stage, and risk score were independent risk factors for BRCA (Fig. 5H). Multivariate independent prognosis analysis revealed that age, stage, and risk score were independent risk factors for BRCA (Fig. 5I). Therefore, to better predict the prognosis of patients with BRCA, a nomogram was constructed based on age, stage, and risk score (Fig. 6A). The calibration curve showed that the nomogram could accurately predict the 3-year, 5-year, and 10-year OSs of patients with BRCA (Fig. 6B). Moreover, decision curve analysis suggested that the predictive value of the risk score was superior to

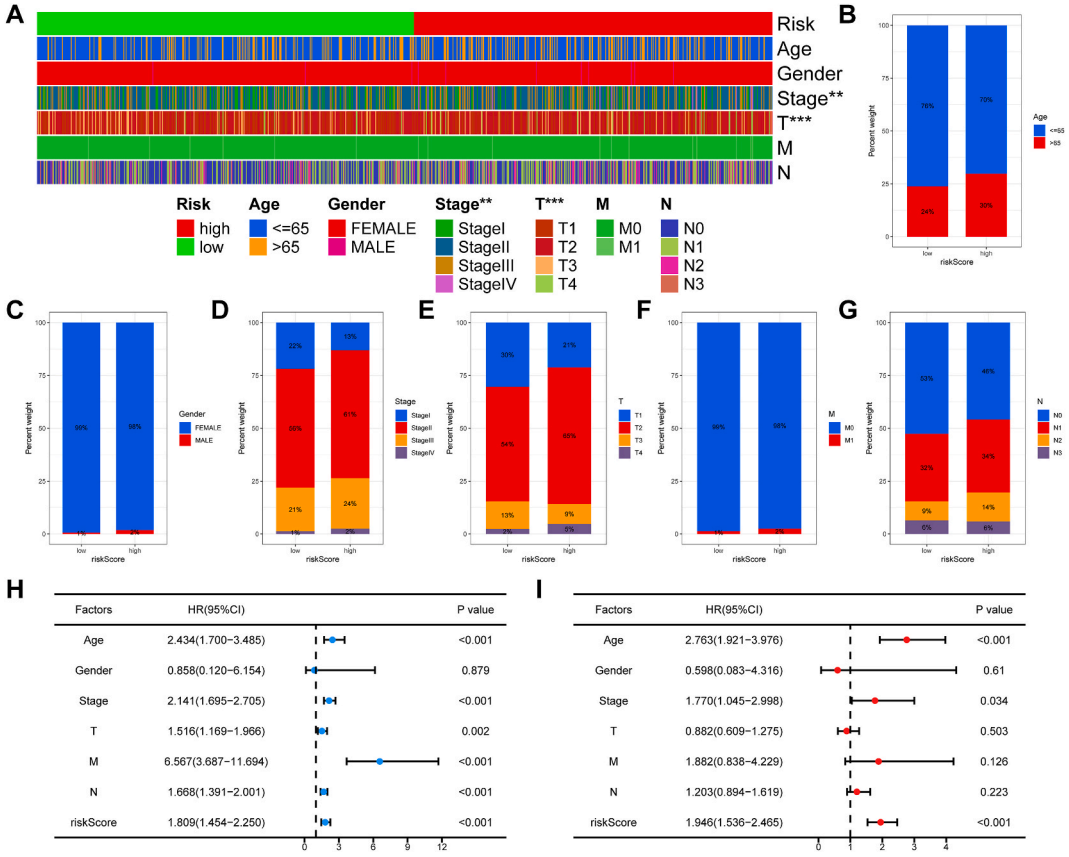

Fig. 5. Validation of the predictive value of the NKRGs-based risk model in the breast cancer cohort. (A) Correlation analysis between clinical characteristics and different risk groups; Correlation analysis between different risk groups and age (B), gender (C), stage (D), T stage (E), M stage (F), and N stage (G). (H) Univariate independent prognosis analysis based on age, gender, stage, T stage, N stage, M stage, and risk score. (I) Multivariate independent prognosis analysis based on age, gender, stage, T stage, N stage, M stage, and risk score. Data are analyzed by Wilcoxon test.

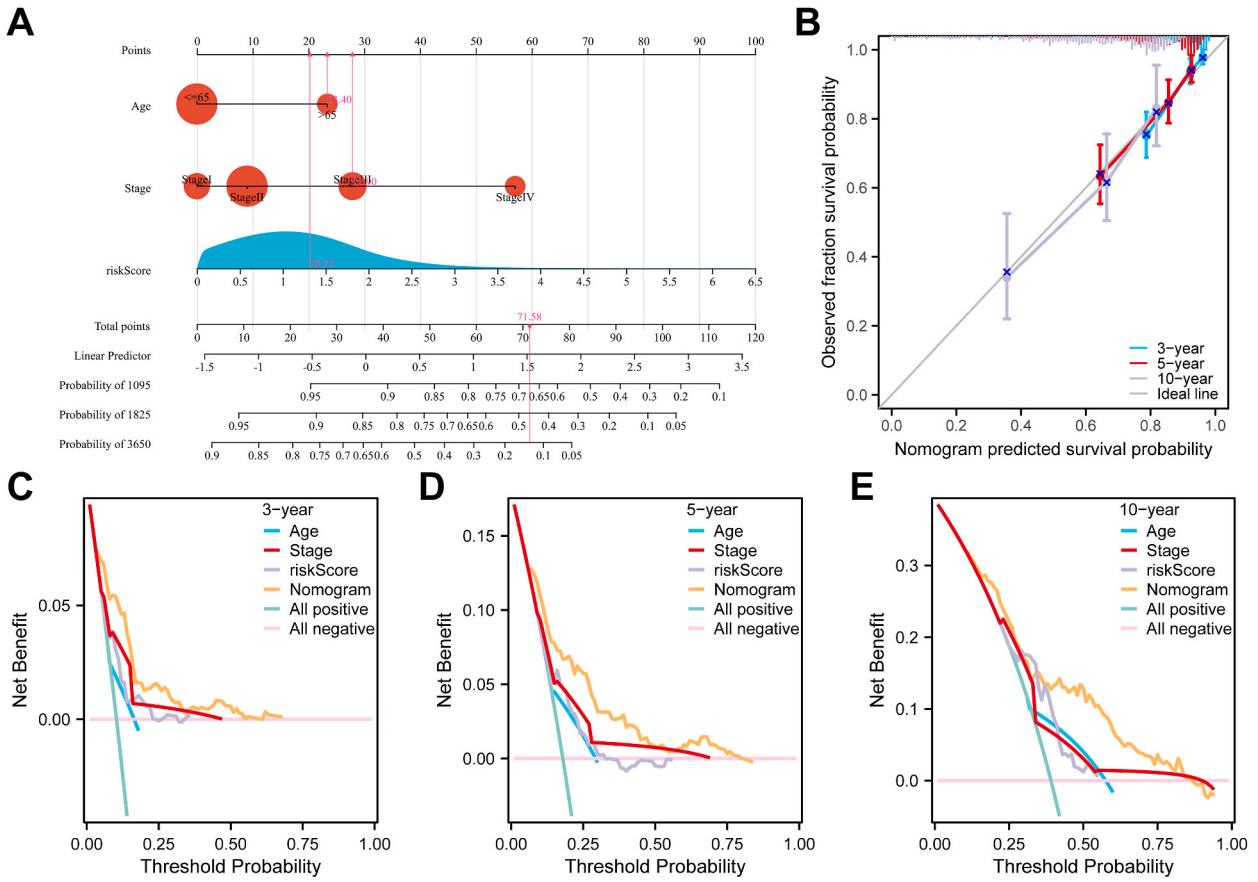

Fig. 6. Nomogram based on the NKRGs-based risk model and clinical characteristics. (A) Nomogram based on the risk score, age, and stage in the breast cancer cohort. (B) Calibration curve showing that the nomogram could well predict the 3-year, 5-year, and 10-year OSs of breast cancer patients; Decision curve analysis for determining the predictive value of the nomogram, risk score, age, and stage for 3-year (C), 5-year (D), and 10-year (E) OSs.

that of age, stage, and risk score (Fig. 6C–E).

3.5. The NKRG-based prognostic prediction model may be a potential biomarker for patients with BRCA

Using various algorithms, positive and negative correlations between immune-related indexes and risk scores were successfully identified. Overall, M0 macrophages, M2 macrophages, neutrophils, and CD4 T cells were positively correlated with the risk score. Contrarily, B cells, CD8 T cells, and mast cells were negatively correlated with the risk score (Fig. 7A, Table S8). In addition, some immune-related functions, such as APC co-inhibition, APC co-stimulation, checkpoint, and HLA, were found to be closely associated with the risk score (Fig. 7B). Numerous immune checkpoint-related genes were found to be highly expressed in the low-risk group, suggesting that patients with BRCA in the low-risk group were likely to gain benefit from immune checkpoint therapy (Fig. 7C). In addition, patients in the low-risk group and high-risk group showed different sensibilities to the positive or negative of CTLA4 and PD1 therapy (Fig. 8A–D).

Moreover, the correlation between TME scores and different risk groups was evaluated. Patients with higher risk scores were found to have lower stromal scores, immune scores, and estimate scores (Fig. 8E). Then, GO and KEGG pathway enrichment analyses were performed based on the differentially expressed NKRGs, and the enrichment of many immune-related pathways was identified. In the GO pathway enrichment analysis, the antigen receptor-mediated signaling pathway, leukocyte-mediated immunity, T cell receptor complex, antigen binding, and immunoglobulin receptor binding were the most enriched pathways (Fig. 8F, Table S9). In the KEGG pathway enrichment analysis, hematopoietic cell lineage, primary immunodeficiency, and cytokine-cytokine receptor interaction were the most enriched pathways (Fig. 8G, Table S10). Subsequently, a positive correlation between tumor mutation burden and risk score was observed (Fig. 8H–I). Survival analysis demonstrated that the OS of patients with BRCA was closely associated with the tumor mutation burden. This finding indicates that patients with a high tumor mutation burden are likely to have poorer OS (Fig. 8J). Moreover, the combination of tumor mutation burden and risk score could accurately predict the prognosis of patients with BRCA (Fig. 8K).

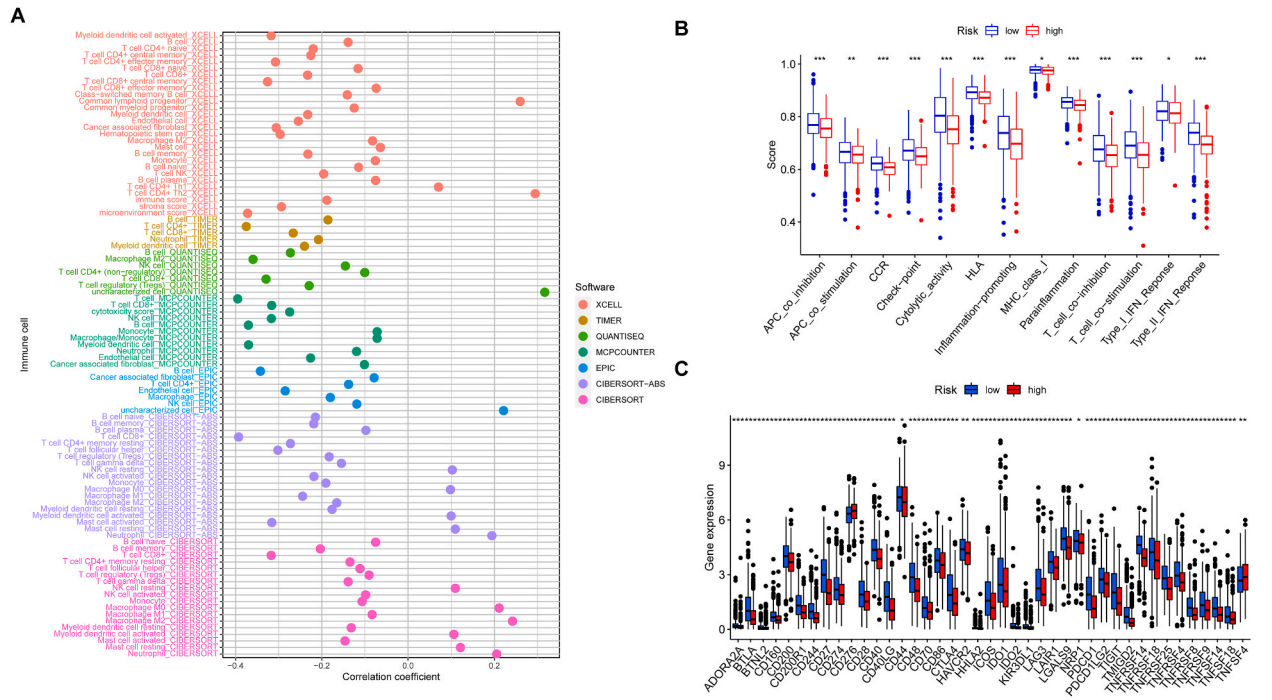

Fig. 7. Correlation between the NKRGs-based risk model and immune cells, immune checkpoint-related genes, and immune-related functions. (A) Immune cell infiltration analysis based on the several algorithms, including TIMER, xCell, MCP-counter, CIBERSORT, EPIC, CIBERSORT-ABS, and quantIseq. (B) Correlation analysis between immune-related functions and risk score. (C) Correlation analysis between immune checkpoint-related genes and risk score. Data are analyzed by Wilcoxon test.

3.6. IFNE expression and prognosis in BRCA

Fig. 9 shows that IFNE is downregulated in BRCA tissues and cell lines and is associated with a good prognosis. To determine whether IFNE is downregulated in BRCA, the expression levels of IFNE in BRCAs and pair-matched adjacent breast normal tissues were examined using RT-qPCR. The expression levels of IFNE were significantly ($p < 0.01$) reduced in the BRCAs compared with those in the normal tissues (Fig. 9A), which is consistent with the results obtained by TIMER 2.0 (Fig. 9D).

The expression levels of IFNE were also investigated in the BRCA cell lines MDA-MB-231, BT-549, ZR-75-1, MCF-7 and SK-BR-3, in which the expression levels were significantly lower compared with those in the normal breast cell line Hs 578Bst (Fig. 9B). In addition, Kaplan-Meier survival analysis showed that low IFNE expression is associated with poor OS in patients with BRCA ($P < 0.05$; Fig. 9C).

3.7. Role of IFNE in BRCA cells

Further analysis based on our NKRG-based risk model demonstrated that IFNE may be a key biomarker in the BRCA cohort. To evaluate the proliferation and invasion abilities of IFNE in BRCA cells, a plasmid was transfected into BT-549 and MDA-MB-231 cells to construct a stable cell line overexpressing IFNE. The IFNE protein expression level was measured via Western blot analysis (Figs. 10A and 11A). Additionally, the EdU assay was performed, demonstrating that IFNE overexpression could significantly reduce the number of EdU-positive BRCA cells ($p < 0.0001$, $p < 0.0001$; Figs. 10B and 11C). Further, the CCK8 assay demonstrated that IFNE overexpression could inhibit the proliferation ability of BRCA cells ($p < 0.0001$; Fig. 10C). The colony formation assay confirmed that IFNE overexpression could suppress BRCA progression ($p < 0.0001$, $p < 0.0001$; Figs. 10D and 11B). Annexin VFITC/PI staining evidently revealed that IFNE overexpression significantly increased the proportion of apoptotic cells ($p < 0.001$; Fig. 10E). Subsequently, the effects of IFNE overexpression on the migratory and invasive capacities of BRCA cells were assessed. Scratch wound healing assay results reflected that IFNE overexpressing BT-549 or MDA-MB-231 cells had significantly impaired migration compared with vector group cells ($p < 0.001$, $p < 0.0001$; Figs. 10G and 11D). Consistently, results of the transwell assay with and without matrigel also showed that IFNE overexpression dramatically suppressed the migration and invasion of BT-549 and MDA-MB-231 cells ($p < 0.0001$, $p < 0.0001$, $p < 0.0001$, $p < 0.0001$; Fig. 10F, H and Fig. 11E and F).

4. Discussion

BRCA is the most common cancer among women, with 1.7 million people diagnosed worldwide and approximately half a million people deaths from this disease each year [25]. The risk of BRCA can be reduced through lifestyle changes, chemoprevention, and

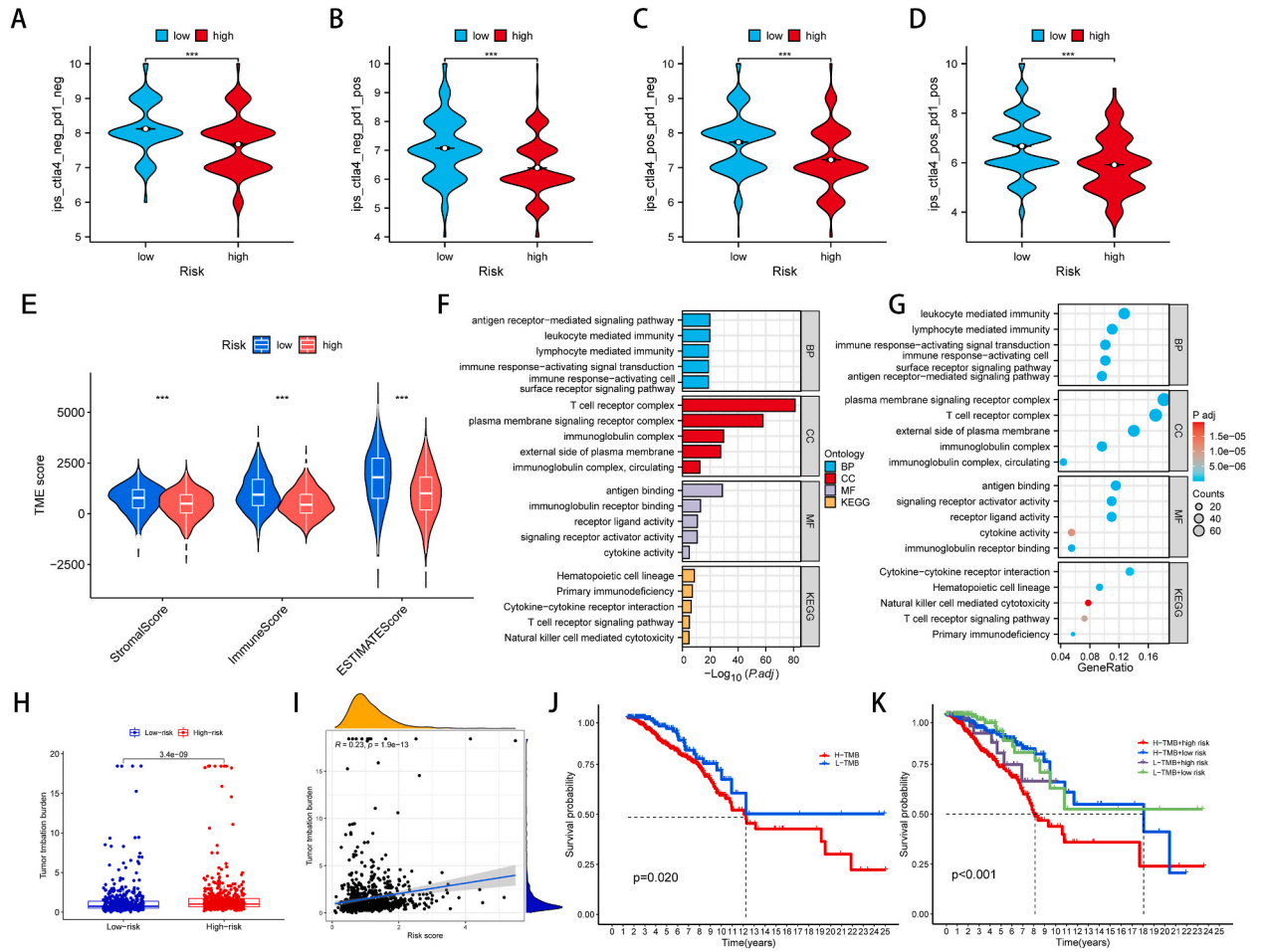

Fig. 8. Correlation between the NKRGs-based risk model and somatic mutations, enriched pathways, immunotherapy, and TMB. (A) Immunotherapy-based comparison of CTLA4-negative and PD1-negative patients between low- and high-risk groups. (B) Immunotherapy-based comparison of CTLA4-negative and PD1-positive patients between low- and high-risk groups. (C) Immunotherapy-based comparison of CTLA4-positive and PD1-negative patients between low- and high-risk groups. (D) Immunotherapy-based comparison of CTLA4-positive and PD1-positive patients between low- and high-risk groups. (E) Correlation analysis between risk score and stromal score, immune score, and estimate score. (F, G) GO and KEGG enrichment analyses based on differentially expressed NKRGs. (H) Boxplot demonstrating the tumor mutation burden in low- and high-risk groups. (I) Correlation analysis between tumor mutation burden and risk score. (J) Survival analysis comparison between low- and high-tumor mutation burden groups. (K) Survival analysis comparison between low- and high-tumor mutation burden groups and low- and high-risk groups. Data are analyzed by Wilcoxon test.

preventive surgery [26]. Despite the development of multiple treatments, BRCA incidence remains high. Therefore, there is an urgent need to identify novel effective therapies for BRCA. A recent study has found that NK cells can regulate immune responses by producing cytokines, which have been applied in the treatment of various types of cancer [27]. Over the recent years, with the development of bioinformatics, there has been more and more research searching for cancer biomarkers. In the present study, 24 prognosis-related NKRGs were identified in a BRCA cohort. Subsequently, based on the expression levels of these 24 prognosis-related NKRGs, the BRCA cohort was successfully divided into two clusters. Analysis of relationships between these NKRGs and clinical characteristics, immune cell infiltration, and somatic mutations as well as pathway enrichment analysis proved that NKRGs play a key role in BRCA and might provide new avenues for developing future therapies. Moreover, NK cells are of great importance to BRCA. One study showed that the PI3K/Akt/GSK-3β/ROS/eIF2B pathway regulates the activity of NK cells and the sensitivity of tumor cells to NK cells, contributing to BRCA growth and lung metastasis [28]. Another study discovered that GARP inhibition promotes the metabolism and function of NK cells, thereby improving the efficacy of NK cell-based immunotherapy [29]. Therefore, the in-depth analysis of key NKRGs may be promising for the diagnosis and treatment of patients with BRCA.

To further explore the key NKRGs that were closely associated with the prognosis of patients with BRCA, LASSO regression analysis and multivariate Cox regression analysis were performed to construct a 4-NKRG-based prognostic model. Using various online datasets, the prognosis and treatment of cancers can now be predicted more precisely. A previous study has examined tumor heterogeneity and organ tropism during BRCA metastasis using transcriptome analyses [30]. Their results have a gained deeper

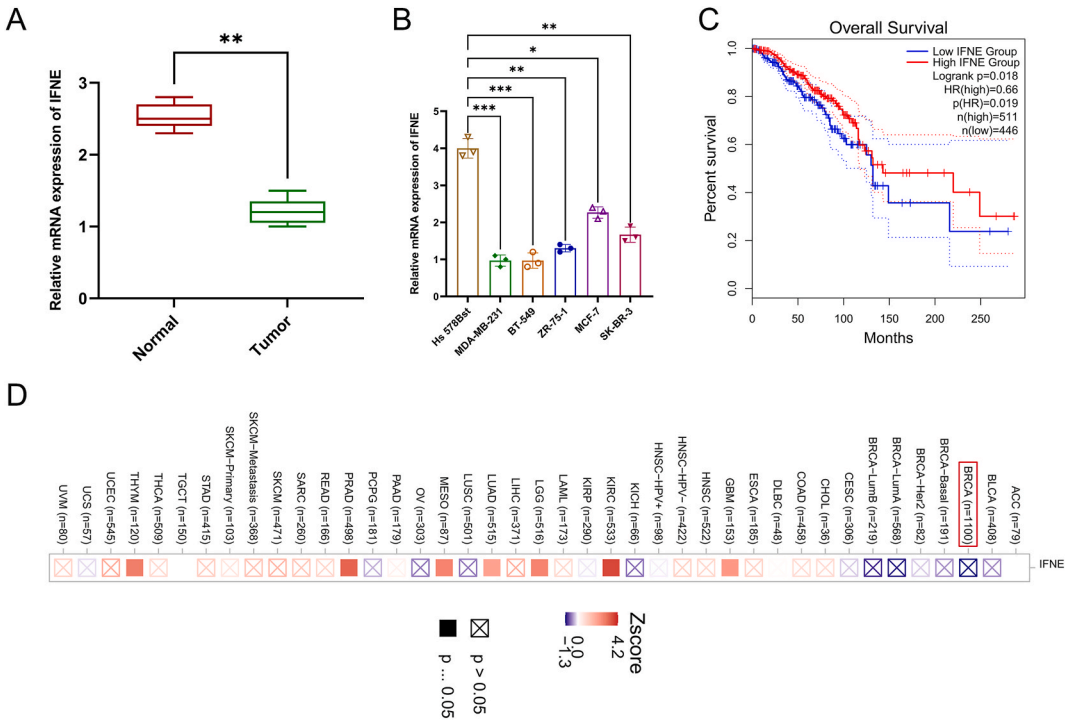

Fig. 9. IFNE expression in breast tumor tissues and cell lines. (A) IFNE expression levels in breast tumor tissues and adjacent normal tissues. (B) IFNE expression in the breast tumor cell lines MDA-MB-231, BT-549, ZR-75-1, MCF-7 and SK-BR-3, and in the normal breast cell line Hs 578Bst. (C) The survival analysis of IFNE expression and overall survival in breast tumor. (D) Expression of IFNE in different tumors. **p < 0.01, ***p < 0.001. Data are analyzed by two-tailed unpaired Student's *t*-test or Wilcoxon test.

understanding of the metastatic progression of BRCA and revealed new targets for BRCA therapy. In addition, genetic markers for BRCA can be utilized to examine how tumor heterogeneity affects metastasis [31].

Different clusters and different risk groups of patients with BRCA showed great correlations with immunotherapy. With the development of immunotherapy, many types of tumors have been treated with immunotherapy to improve the prognosis. Immunotherapy seems to be revolutionizing the management of multiple solid tumors [32]. BRCA treatment has long used monoclonal antibodies, such as trastuzumab, a passive immunotherapy, as therapeutic agents [33]. To maximize antitumor immunity, antibody-drug conjugates serve as another novel therapy. They contain tumor-specific mAbs covalently bound to cytotoxins. To select patients most likely to benefit from immunotherapy, biomarkers that can predict clinical outcomes are needed [34]. In the present work, four NKRGs — IFNE, PRDX1, RAC2, and ULBP2 — that may provide a new direction for immunotherapy in patients with BRCA, were identified. This four NKRG-based prognostic model could accurately predict the immune response in the BRCA cohort. Moreover, the NKRG-based risk model was also closely associated with the clinical characteristics of patients with BRCA, such as stage and T stage. The univariate and multivariate Cox regression analyses demonstrated that the NKRG-based risk model was an independent prognostic factor in BRCA. The nomogram in our study was constructed based on the age, stage, and risk score, and the calibration curve demonstrated that the nomogram could well predict the 3-year, 5-year, and 10-year OSs of patients with BRCA.

The GO enrichment analysis conducted in the present study revealed that numerous immune-related pathways were significantly enriched in the four-NKRG risk model, such as antigen receptor-mediated signaling pathway, leukocyte-mediated immunity, T cell receptor complex, antigen binding, and immunoglobulin receptor binding. The onset, progression, and control of BRCA are strongly influenced by the immune system. Immunoediting is characterized by the evolving interaction between BRCAs and host immunity. As BRCA progresses, acute inflammation triggers the activation of innate immunity, resulting in cancer cell death and the maturation of dendritic cells, which activate T cells specifically targeting BRCA [35–37]. Either immune-mediated rejection of early-stage tumors or selection of tumor cell variants that can escape the immune response occurs at this stage [38]. The use of immunotherapy has extended survival in patients with other solid tumors besides BRCA and is thus a promising therapeutic approach. Immune checkpoint inhibitors, which block immunosuppressive receptors, have proven to be among the most effective immunotherapeutic drugs [39,40]. Moreover, immunotherapy has been widely applied in the field of BRCA. According to an early report on PD-1/PD-L1 antagonists, some BRCA cases are intrinsically immunogenic, with some responding patients showing durable clinical responses [41]. It is estimated that less than 10 % of patients with metastatic cancer have single-agent activity [42,43]. Therefore, it is urgent to identify potential biomarkers that can guide immunotherapy in patients with BRCA. In the present work, an NKRG-based risk model was successfully constructed. The IPS scoring suggested that patients with lower risk scores tended to be more responsive to immunotherapy, which indicates that the NKRGs on which these risk scores are based might be effective biomarkers for patients with BRCA.

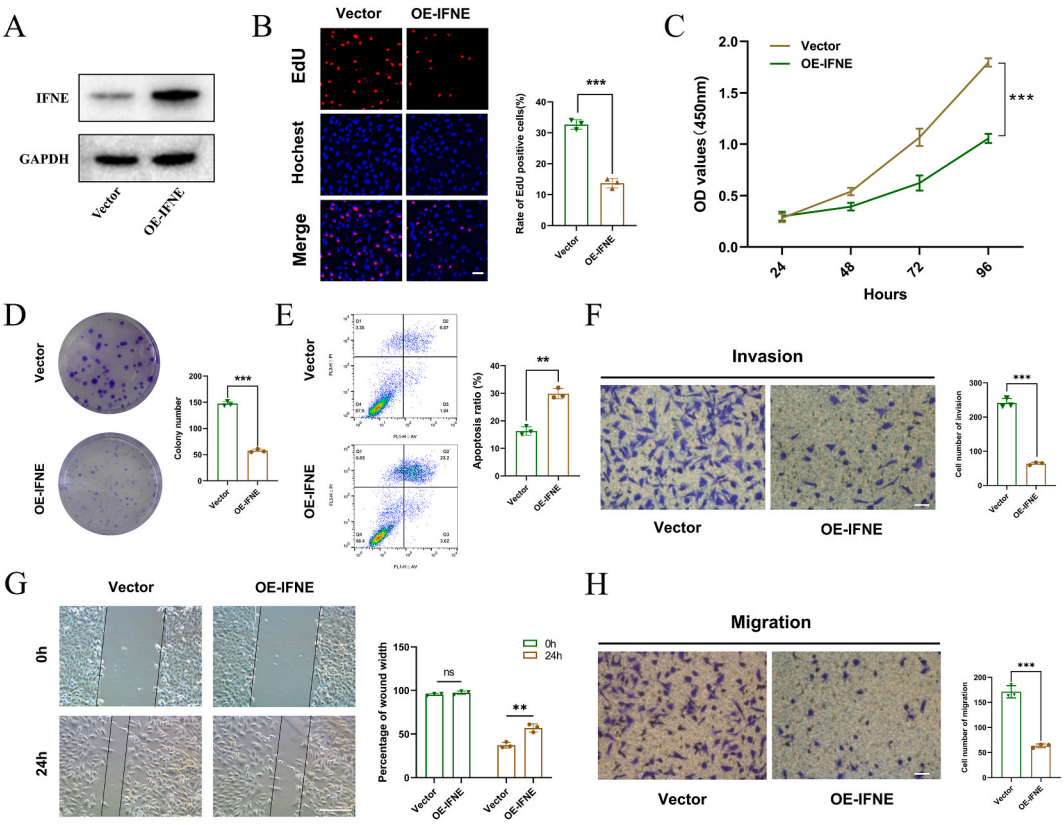

Fig. 10. (A) Construction of a stable IFNE overexpressing BT-549 cell line and verification via Western blot analysis. Proliferation and clonogenic capacities of BT-549/OE-IFNE cells and BT-549/Vector cells were examined via the EdU assay (B), cell counting kit-8 assay (C), and colony formation assay (D). (E) Cell apoptosis rate assessment using flow cytometric analysis combined with Annexin V-FITC/PI staining. (G) Wound healing assay of BT-549 cells, experiments were terminated 24 h after scratching. Effect of IFNE overexpression on breast cancer cell invasion (F) and migration (H) based on transwell assays. OE-IFNE cells: IFNE overexpressing cells; $^{**}p < 0.01$, $^{***}p < 0.001$ (Fig. B scare bar:100 μm; Fig. F,H scare bar:50 μm; Fig G scare bar:200 μm) . Data are analyzed by two-tailed unpaired Student's *t*-test or Wilcoxon test.

Finally, to evaluate the role of key NKRGs in BRCA cells, cell proliferation and invasion assays were performed for IFNE. IFNE overexpression could significantly suppress cell proliferation and invasion abilities in BRCA cells. The IFNE, or Interferon Epsilon, is a protein-coding gene. Its related pathways include those involving interferons and the DDX58/IFIH1-mediated induction of interferons during cancer development. The IFNE gene ontology (GO) analysis indicated the activity of cytokines and binding of type I interferon receptors. However, the role of IFNE in BRCA has not been studied previously. Cell migration is a complex process essential for various physiological and pathological conditions. Interferons (IFNs), including IFNE, are known to influence this process, although the mechanisms can vary depending on the cell type and context [44]. Upon binding to its receptor, IFNE activates the JAK-STAT signaling pathway. This pathway is critical in transmitting the signal from the cell surface to the DNA in the nucleus, ultimately influencing gene expression. IFNE can influence the expression of certain genes involved in promoting or inhibiting the cell cycle. For example, it can upregulate the expression of cell cycle inhibitors (like p21) that halt the cell cycle, reducing cell proliferation [45].

PRDX1 is known for its role in reducing hydrogen peroxide levels, thereby regulating oxidative stress within cells [46]. In the context of cancer, oxidative stress has been implicated in various stages of cancer progression, from DNA mutation to cancer cell proliferation and survival. Although we did not directly assess PRDX1 in our experiments, its regulation in immune cells and cancer cells suggests a dual role. By maintaining redox balance, PRDX1 may prevent DNA damage and mutations; conversely, its antioxidant function may support cancer cell survival by protecting against immune cell-induced oxidative stress [47]. This dichotomy warrants further exploration, especially concerning BRCA's oxidative environment. RAC2, a member of the Rho GTPase family, is primarily expressed in hematopoietic cells and is crucial for the regulation of the immune response, including the release of reactive oxygen species (ROS) and the organization of the actin cytoskeleton in immune cells. While our study did not explore RAC2, its known involvement in cellular processes like migration, ROS production, and phagocytosis in immune cells makes it a candidate of interest in cancer immunotherapy [48]. For instance, alterations in RAC2 expression or activity could influence immune surveillance and the TME in BRCA [49]. ULBP2 is one of the ligands for the NKG2D receptor expressed in NK cells and certain T cells [50]. It is known to be induced by stress and is often upregulated in cancerous cells, signaling them for elimination by the immune system [51].

However, the study has some limitations. First, the clinical cohorts of patients with BRCA analyzed in our study were exclusively acquired from the TCGA and GSE42568. The 4-NKRG-based prognostic model also needs to be validated by external large cohorts.

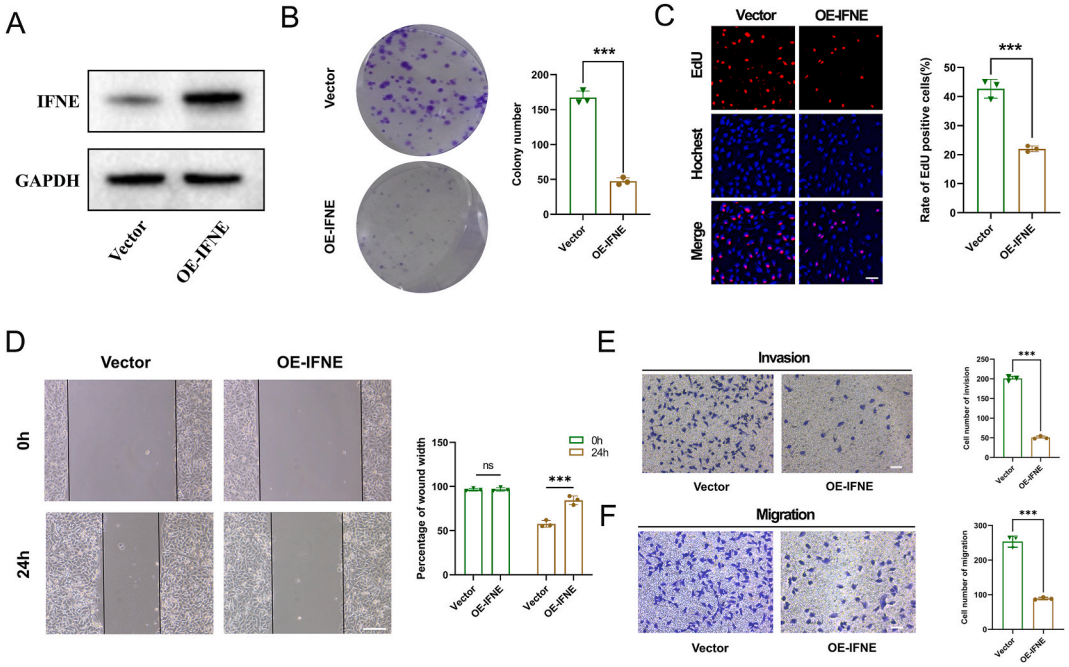

Fig. 11. (A) Construction of a stable IFNE overexpressing MDA-MB-231 cell line and verification via Western blot analysis. Proliferation and clonogenic capacities of MDA-MB-231/OE-IFNE cells and MDA-MB-231/Vector cells were examined via colony formation assay (B) and EdU assay (C). (D) Wound healing assay of MDA-MB-231cells, experiments were terminated 24 h after scratching. Effect of IFNE overexpression on breast cancer cell invasion (E) and migration (F) based on transwell assays. OE-IFNE cells: IFNE overexpressing cells; $^{**}p < 0.01$, $^{***}p < 0.001$ (Fig. C scare bar:100 μm; Fig D scare bar:200 μm; Fig. E,F scare bar:50 μm) . Data are analyzed by two-tailed unpaired Student's *t*-test or Wilcoxon test.

Second, an in-depth characterization of the mechanisms of IFNE in BRCA is required through animal experiments. Furthermore, the functions of the other three markers, including PRDX1, RAC2, and ULBP2, should be explored *in vivo* and *in vitro* in the future.

5. Conclusion

This study developed a novel 4-NKRG prognostic model and nomogram capable of predicting the prognosis of patients with BRCA. Additionally, the prognostic model was found to be closely associated with the immune microenvironment, opening new therapeutic avenues for cancer.

Data availability statement

Data associated with the study has been deposited at TCGA and GEO under the accession number GSE42568. All the experimental data analyzed in the study are available from the corresponding author upon the reasonable request.

Ethical approval

Since all the data used in the current study was available online, and no individual patient was involved, the IRB (Institutional Review Board) review was exempted.

Funding

The project Supported by the Youth Fund of the Natural Science Foundation of Jiangxi Province of China (20224BAB216064) and Natural Science Foundation of Jiangxi Province of China (20224BAB206075).

CRediT authorship contribution statement

Dongmin Yu: Funding acquisition, Data curation, Conceptualization. **Chao Huang:** Software, Project administration, Formal analysis. **Luochen Zhu:** Writing – original draft, Visualization. **Yuxi Wei:** Writing – review & editing, Methodology, Investigation. **Meifang Li:** Visualization, Supervision, Funding acquisition.

Declaration of competing interest

The authors declare that they have no known competing financial interests or personal relationships that could have appeared to influence the work reported in this paper.

Appendix A. Supplementary data

Supplementary data to this article can be found online at https://doi.org/10.1016/j.heliyon.2023.e23930.

References

[1] K.S. Peairs, Y. Choi, R.W. Stewart, H.F. Sateia, Screening for breast cancer, Semin. Oncol. 44 (2017) 60–72.
[2] T. Schmidt, M. van Mackelenbergh, D. Wesch, C. Mundhenke, Physical activity influences the immune system of breast cancer patients, J. Cancer Res. Therapeut. 13 (2017) 392–398.
[3] M.A. B, V.R. S, M.J. E, A.A. O, Breast cancer biomarkers: risk assessment, diagnosis, prognosis, prediction of treatment efficacy and toxicity, and recurrence, Curr. Pharmaceut. Des. 20 (2014) 4879–4898.
[4] Z. Anastasiadi, G.D. Lianos, E. Ignatiadou, H.V. Harissis, M. Mitsis, Breast cancer in young women: an overview, Updates Surg 69 (2017) 313–317.
[5] U. Veronesi, P. Boyle, A. Goldhirsch, R. Orecchia, G. Viale, Breast cancer, Lancet 365 (2005) 1727–1741.
[6] T.G. Odle, Precision medicine in breast cancer, Radiol. Technol. 88 (2017) 401m–421m.
[7] K. Barzaman, J. Karami, Z. Zarei, A. Hosseinzadeh, M.H. Kazemi, S. Moradi-Kalbolandi, E. Safari, L. Farahmand, Breast cancer: biology, biomarkers, and treatments, Int. Immunopharm. 84 (2020), 106535.
[8] G. Zheng, Z. Guo, W. Li, W. Xi, B. Zuo, R. Zhang, W. Wen, A.G. Yang, L. Jia, Interaction between HLA-G and NK cell receptor KIR2DL4 orchestrates HER2-positive breast cancer resistance to trastuzumab, Signal Transduct. Targeted Ther. 6 (2021) 236.
[9] A.L. Correia, J.C. Guimaraes, P. Auf der Maur, D. De Silva, M.P. Trefny, R. Okamoto, S. Bruno, A. Schmidt, K. Mertz, K. Volkmann, L. Terracciano, A. Zippelius, M. Vetter, C. Kurzeder, W.P. Weber, M. Bentires-Alj, Hepatic stellate cells suppress NK cell-sustained breast cancer dormancy, Nature 594 (2021) 566–571.
[10] Y. Gong, W. Chen, X. Chen, Y. He, H. Jiang, X. Zhang, L. Pan, B. Ni, F. Yang, Y. Xu, Q. Zhang, L. Zhou, Y. Cheng, An injectable epigenetic autophagic modulatory hydrogel for boosting umbilical cord blood NK cell therapy prevents postsurgical relapse of triple-negative breast cancer, Adv. Sci. 9 (2022), e2201271.
[11] S. Rezaeifard, A. Talei, M. Shariat, N. Erfani, Tumor infiltrating NK cell (TINK) subsets and functional molecules in patients with breast cancer, Mol. Immunol. 136 (2021) 161–167.
[12] F. Jin, Z. Wu, X. Hu, J. Zhang, Z. Gao, X. Han, J. Qin, C. Li, Y. Wang, The PI3K/Akt/GSK-3β/ROS/eIF2B pathway promotes breast cancer growth and metastasis via suppression of NK cell cytotoxicity and tumor cell susceptibility, Cancer Biol Med 16 (2019) 38–54.
[13] K. Slattery, E. Woods, V. Zaiatz-Bittencourt, S. Marks, S. Chew, M. Conroy, C. Goggin, C. MacEochagain, J. Kennedy, S. Lucas, D.K. Finlay, C.M. Gardiner, TGFβ drives NK cell metabolic dysfunction in human metastatic breast cancer, J Immunother Cancer 9 (2021).
[14] A.M. Coletta, N.H. Agha, F.L. Baker, G.M. Niemiro, P.L. Mylabathula, A.M. Brewster, T.B. Bevers, E. Fuentes-Mattei, K. Basen-Engquist, S.C. Gilchrist, R. J. Simpson, The impact of high-intensity interval exercise training on NK-cell function and circulating myokines for breast cancer prevention among women at high risk for breast cancer, Breast Cancer Res. Treat. 187 (2021) 407–416.
[15] Z. Hong, Y. Li, X. Deng, M. Chen, J. Pan, Z. Chen, X. Zhang, C. Wang, C. Qiu, Comprehensive analysis of triphenyl phosphate: an environmental explanation of colorectal cancer progression, Ecotoxicol. Environ. Saf. 241 (2022), 113778.
[16] T. Zhang, J. Wu, X. Zhang, X. Zhou, S. Wang, Z. Wang, Pharmacophore based in silico study with laboratory verification-environmental explanation of prostate cancer recurrence, Environ. Sci. Pollut. Res. Int. 28 (2021) 61581–61591.
[17] S. Ye, Q. Liu, K. Huang, X. Jiang, X. Zhang, The comprehensive analysis based study of perfluorinated compounds-Environmental explanation of bladder cancer progression, Ecotoxicol. Environ. Saf. 229 (2022), 113059.
[18] T. Li, J. Fu, Z. Zeng, et al., TIMER2.0 for analysis of tumor-infiltrating immune cells, Nucleic Acids Res. 48 (W1) (2020) W509–W514, https://doi.org/10.1093/nar/gkaa407.
[19] D. Aran, Cell-type enrichment analysis of bulk transcriptomes using xCell, Methods Mol. Biol. 2120 (2020) 263–276, https://doi.org/10.1007/978-1-0716-0327-7_19.
[20] R. Dienstmann, G. Villacampa, A. Sveen, et al., Relative contribution of clinicopathological variables, genomic markers, transcriptomic subtyping and microenvironment features for outcome prediction in stage II/III colorectal cancer, Ann. Oncol. 30 (10) (2019) 1622–1629, https://doi.org/10.1093/annonc/mdz287.
[21] H. Zhang, R. Li, Y. Cao, et al., Poor clinical outcomes and immunoevasive contexture in intratumoral IL-10-producing macrophages enriched gastric cancer patients, Ann. Surg. 275 (4) (2022), e626-e635, https://doi.org/10.1097/SLA.0000000000004037.
[22] J. Racle, K. de Jonge, P. Baumgaertner, D.E. Speiser, D. Gfeller, Simultaneous enumeration of cancer and immune cell types from bulk tumor gene expression data, Elife 6 (2017), e26476, https://doi.org/10.7554/eLife.26476. Published 2017 Nov 13.
[23] M. Tamminga, T.J.N. Hiltermann, E. Schuuring, W. Timens, R.S. Fehrmann, H.J. Groen, Immune microenvironment composition in non-small cell lung cancer and its association with survival, Clin Transl Immunology 9 (6) (2020), e1142, https://doi.org/10.1002/cti2.1142. Published 2020 Jun 12.
[24] F. Finotello, C. Mayer, C. Plattner, et al., Molecular and pharmacological modulators of the tumor immune contexture revealed by deconvolution of RNA-seq data [published correction appears in Genome Med. 2019 Jul 29;11(1):50], Genome Med. 11 (1) (2019) 34, https://doi.org/10.1186/s13073-019-0638-6. Published 2019 May 24.
[25] Z. Li, L. Chen, C. Chen, Y. Zhou, D. Hu, J. Yang, Y. Chen, W. Zhuo, M. Mao, X. Zhang, L. Xu, L. Wang, J. Zhou, Targeting ferroptosis in breast cancer, Biomark. Res. 8 (1) (2020 Nov 5) 58, https://doi.org/10.1186/s40364-020-00230-3. PMID: 33292585; PMCID: PMC7643412.
[26] X. Li, J. Yang, L. Peng, A.A. Sahin, L. Huo, K.C. Ward, R. O'Regan, M.A. Torres, J.L. Meisel, Triple-negative breast cancer has worse overall survival and cause-specific survival than non-triple-negative breast cancer, Breast Cancer Res. Treat. 161 (2017) 279–287.
[27] R. Tallerico, L. Conti, S. Lanzardo, R. Sottile, C. Garofalo, A.K. Wagner, M.H. Johansson, C.M. Cristiani, K. Kärre, E. Carbone, F. Cavallo, NK cells control breast cancer and related cancer stem cell hematological spread, OncoImmunology 6 (2017), e1284718.
[28] Z. Chen, Z. Zeng, Q. Wan, X. Liu, J. Qi, Y. Zu, Targeted immunotherapy of triple-negative breast cancer by aptamer-engineered NK cells, Biomaterials 280 (2022), 121259.
[29] L. Besson, B. Mery, M. Morelle, Y. Rocca, P.E. Heudel, B. You, T. Bachelot, I. Ray-Coquard, M. Villard, E. Charrier, F. Parant, S. Viel, G. Garin, R. Mayet, D. Perol, T. Walzer, O. Tredan, A. Marçais, Cutting edge: mTORC1 inhibition in metastatic breast cancer patients negatively affects peripheral NK cell maturation and number, J. Immunol. 206 (2021) 2265–2270.
[30] T. Bonacho, F. Rodrigues, J. Liberal, Immunohistochemistry for diagnosis and prognosis of breast cancer: a review, Biotech. Histochem. 95 (2020) 71–91.
[31] G. Li, J. Hu, G. Hu, Biomarker studies in early detection and prognosis of breast cancer, Adv. Exp. Med. Biol. 1026 (2017) 27–39.
[32] L.A. Emens, Breast cancer immunotherapy: facts and hopes, Clin. Cancer Res. 24 (2018) 511–520.
[33] T.E. Keenan, S.M. Tolaney, Role of immunotherapy in triple-negative breast cancer, J Natl Compr Canc Netw 18 (2020) 479–489.

[34] A. Costa, Y. Kieffer, A. Scholer-Dahirel, F. Pelon, B. Bourachot, M. Cardon, P. Sirven, I. Magagna, L. Fuhrmann, C. Bernard, C. Bonneau, M. Kondratova, I. Kuperstein, A. Zinovyev, A.M. Givel, M.C. Parrini, V. Soumelis, A. Vincent-Salomon, F. Mechta-Grigoriou, Fibroblast heterogeneity and immunosuppressive environment in human breast cancer, Cancer Cell 33 (2018) 463–479, e410.
[35] I. Erić, A. Petek Erić, J. Kristek, I. Koprivčić, M. Babić, Breast cancer in young women: pathologic and immunohistochemical features, Acta Clin. Croat. 57 (2018) 497–502.
[36] M.V. Dieci, F. Miglietta, V. Guarneri, Immune infiltrates in breast cancer: recent updates and clinical implications, Cells 10 (2021).
[37] S. Yu, W. Li, L. Tang, X. Fan, S. Yao, X. Zhang, Z. Bi, H. Cheng, Depression in breast cancer patients: immunopathogenesis and immunotherapy, Cancer Lett. 536 (2022), 215648.
[38] L.A. Emens, Immunotherapy in triple-negative breast cancer, Cancer J. 27 (2021) 59–66.
[39] E. Mezni, K. Behi, A. Gonçalves, Immunotherapy and breast cancer: an overview, Curr. Opin. Oncol. 34 (2022) 587–594.
[40] H.C. Regen-Tuero, R.C. Ward, W.M. Sikov, P.J. Littrup, Cryoablation and immunotherapy for breast cancer: overview and rationale for combined therapy, Radiol Imaging Cancer 3 (2021), e200134.
[41] V. Yaghoobi, S. Martinez-Morilla, Y. Liu, L. Charette, D.L. Rimm, M. Harigopal, Advances in quantitative immunohistochemistry and their contribution to breast cancer, Expert Rev. Mol. Diagn 20 (2020) 509–522.
[42] E. Quaglino, L. Conti, F. Cavallo, Breast cancer stem cell antigens as targets for immunotherapy, Semin. Immunol. 47 (2020), 101386.
[43] J.P. Bates, R. Derakhshandeh, L. Jones, T.J. Webb, Mechanisms of immune evasion in breast cancer, BMC Cancer 18 (2018) 556.
[44] D. Jorgovanovic, M. Song, L. Wang, Y. Zhang, Roles of IFN-γ in tumor progression and regression: a review, Biomark. Res. 8 (2020) 49, https://doi.org/10.1186/s40364-020-00228-x. PMID: 33005420; PMCID: PMC7526126.
[45] M.A. Kursunel, G. Esendagli, The untold story of IFN-γ in cancer biology, Cytokine Growth Factor Rev. 31 (2016) 73–81, https://doi.org/10.1016/j.cytogfr.2016.07.005. Epub 2016 Aug 1. Erratum in: Cytokine Growth Factor Rev. 2017 Jun;35:97. PMID: 27502919.
[46] C. Ding, X. Fan, G. Wu, Peroxiredoxin 1 - an antioxidant enzyme in cancer, J. Cell Mol. Med. 21 (1) (2017) 193–202, https://doi.org/10.1111/jcmm.12955. Epub 2016 Sep 21. PMID: 27653015; PMCID: PMC5192802.
[47] S. Smith, Telomerase can't handle the stress, Genes Dev. 32 (9–10) (2018) 597–599, https://doi.org/10.1101/gad.316042.118. PMID: 29802121; PMCID: PMC6004074.
[48] V. Lougaris, M. Baronio, L. Gazzurelli, A. Benvenuto, A. Plebani, RAC2 and primary human immune deficiencies, J. Leukoc. Biol. 108 (2) (2020) 687–696, https://doi.org/10.1002/JLB.5MR0520-194RR. Epub 2020 Jun 15. PMID: 32542921.
[49] A.P. Hsu, Not too little, not too much: the impact of mutation types in Wiskott-Aldrich syndrome and RAC2 patients, Clin. Exp. Immunol. 212 (2) (2023) 137–146, https://doi.org/10.1093/cei/uxad001. PMID: 36617178; PMCID: PMC10128166.
[50] R.A. Youness, A.Z. Gad, K. Sanber, Y.J. Ahn, G.J. Lee, E. Khallaf, H.M. Hafez, A.A. Motaal, N. Ahmed, M.Z. Gad, Targeting hydrogen sulphide signaling in breast cancer, J. Adv. Res. 27 (2020) 177–190, https://doi.org/10.1016/j.jare.2020.07.006. PMID: 33318876; PMCID: PMC7728592.
[51] H. Ding, X. Yang, Y. Wei, Fusion proteins of NKG2D/NKG2DL in cancer immunotherapy, Int. J. Mol. Sci. 19 (1) (2018) 177, https://doi.org/10.3390/ijms19010177. PMID: 29316666; PMCID: PMC5796126.